

**Xavier F. Figueroa, Chien-Chang Chen, Kevin P. Campbell, David N. Damon,
Kathleen H. Day, Susan Ramos and Brian R. Duling**
Am J Physiol Heart Circ Physiol 293:1371-1383, 2007. First published May 18, 2007;
doi:10.1152/ajpheart.01368.2006

You might find this additional information useful...

This article cites 70 articles, 39 of which you can access free at:

<http://ajpheart.physiology.org/cgi/content/full/293/3/H1371#BIBL>

Updated information and services including high-resolution figures, can be found at:

<http://ajpheart.physiology.org/cgi/content/full/293/3/H1371>

Additional material and information about *AJP - Heart and Circulatory Physiology* can be found at:

<http://www.the-aps.org/publications/ajpheart>

This information is current as of July 30, 2008 .

Are voltage-dependent ion channels involved in the endothelial cell control of vasomotor tone?

Xavier F. Figueroa,¹ Chien-Chang Chen,² Kevin P. Campbell,^{3,4,5} David N. Damon,⁶ Kathleen H. Day,⁶ Susan Ramos,⁶ and Brian R. Duling⁶

¹Departamento de Ciencias Fisiológicas, Facultad de Ciencias Biológicas, Pontificia Universidad Católica de Chile, Santiago, Chile; ²Institute of Biomedical Science, Academia Sinica, Nankang, Taipei, Taiwan; ³Howard Hughes Medical Institute and Departments of ⁴Physiology and Biophysics and ⁵Neurology, University of Iowa, Iowa City, Iowa; and ⁶Department of Molecular Physiology and Biological Physics, University of Virginia, Charlottesville, Virginia

Submitted 14 December 2006; accepted in final form 18 May 2007

Figueroa XF, Chen CC, Campbell KP, Damon DN, Day KH, Ramos S, Duling BR. Are voltage-dependent ion channels involved in the endothelial cell control of vasomotor tone? *Am J Physiol Heart Circ Physiol* 293: H1371–H1383, 2007. First published May 18, 2007; doi:10.1152/ajpheart.01368.2006.—In the microcirculation, longitudinal conduction of vasomotor responses provides an essential means of coordinating flow distribution among vessels in a complex network. Spread of current along the vessel axis can display a regenerative component, which leads to propagation of vasomotor signals over many millimeters; the ionic basis for the regenerative response is unknown. We examined the responses to 10 s of focal electrical stimulation (30 Hz, 2 ms, 30 V) of mouse cremaster arterioles to test the hypothesis that voltage-dependent Na⁺ (Na_v) and Ca²⁺ channels might be activated in long-distance signaling in microvessels. Electrical stimulation evoked a vasoconstriction at the site of stimulation and a spreading, nondecremental conducted dilation. Endothelial damage (air bubble) blocked conduction of the vasodilation, indicating an involvement of the endothelium. The Na_v channel blocker bupivacaine also blocked conduction, and TTX attenuated it. The Na_v channel activator veratridine induced an endothelium-dependent dilation. The Na_v channel isoforms Na_v1.2, Na_v1.6, and Na_v1.9 were detected in the endothelial cells of cremaster arterioles by immunocytochemistry. These findings are consistent with the involvement of Na_v channels in the conducted response. BAPTA buffering of endothelial cell Ca²⁺ delayed and reduced the conducted dilation, which was almost eliminated by Ni²⁺, amiloride, or deletion of α_{1H} T-type Ca²⁺ (Ca_v3.2) channels. Blockade of endothelial nitric oxide synthase or Ca²⁺-activated K⁺ channels also inhibited the conducted vasodilation. Our findings indicate that an electrically induced signal can propagate along the vessel axis via the endothelium and can induce sequential activation of Na_v and Ca_v3.2 channels. The resultant Ca²⁺ influx activates endothelial nitric oxide synthase and Ca²⁺-activated K⁺ channels, triggering vasodilation.

conducted vasodilation; T-type calcium channels; hypertension; gap junction; voltage-gated sodium channels

CONTROL OF BLOOD PRESSURE and blood flow depends on the regulation of vessel diameter and on the integrated responses of different segments of the arteriolar resistance network (12, 47, 48). Thus, vascular function depends on precise, well-integrated activation of adjacent smooth muscle and endothelial cells (27, 48, 49), processes that are accomplished, in large part, by cell-cell conduction of electrical signals via gap junctions (12, 16, 20, 27, 50, 62, 65). Vasodilator signals

generated in the endothelium can extend many millimeters along the vessel axis without noticeable decay (12, 14, 16, 17), and such nondecremental conduction suggests the involvement of a regenerative mechanism that would likely require one or more voltage-dependent ion channels. Consistent with this hypothesis, focal electrical stimulation of arterioles with a micropipette activates a vasoconstriction that is restricted to a short vessel segment at the stimulation site and, in addition, causes a nondecremental, conducted vasodilation that is non-neurally mediated and dependent on the presence of connexin 40 (Cx40) (20), a gap junctional protein confined to the endothelium (12, 20). These findings raise two questions: 1) How is a regenerative conduction initiated and/or sustained? 2) How is a conducted electrical signal linked to vasodilation?

Voltage-dependent ion channels are not generally thought to be present in the endothelium, and endothelial cells are typically assumed to be electrically unexcitable (38), but a number of observations suggest otherwise. Electrical field stimulation induces a nonneuronal, endothelium-dependent vasodilation in vitro, and such stimulation can cause nitric oxide (NO) release from cultured endothelial cells (7, 17, 23, 24, 53). Moreover, although not widely appreciated, voltage-dependent Na⁺ (Na_v) and Ca²⁺ (Ca_v) channels have been detected in endothelial cells (2, 3, 21, 25, 26, 55, 57, 58, 61, 63, 66, 70), and these ion channels have been reported to be functional. T-type, voltage-dependent Ca²⁺ (Ca_v3) channels of the sub-type α_{1H} (Ca_v3.2) are essential for normal relaxation of the murine coronary arteries (10), and the Na_v channels are involved in the endothelial response to shear stress (55).

On the basis of the above-described findings, we hypothesized that Na_v and Ca_v channels might be activated in long-distance signaling in microvessels and, thus, could play a role in the regulation of vasomotor tone. Our experiments support the proposition that electrical stimulation induces regenerative activation of endothelial cell Na_v channels. Furthermore, our findings are consistent with the idea that a depolarization induced by opening of Na_v channels leads to activation of endothelial cell Ca_v3.2 channels, providing a key trigger for long-distance, endothelium-dependent activation of NO production and Ca²⁺-activated K⁺ (K_{Ca}) channels, which leads to vasodilation.

Address for reprint requests and other correspondence: B. R. Duling, Dept. of Molecular Physiology and Biological Physics, Univ. of Virginia Health Sciences Center, PO Box 800736, Charlottesville, VA 22908-0736 (e-mail: brd@virginia.edu).

The costs of publication of this article were defrayed in part by the payment of page charges. The article must therefore be hereby marked "advertisement" in accordance with 18 U.S.C. Section 1734 solely to indicate this fact.

MATERIALS AND METHODS

Male C57Bl/6 (wild-type), endothelial NO synthase (eNOS)-knockout (eNOS^{-/-}) (44), α_1 3.2-knockout (α_1 3.2^{-/-}) (10), and β_1 -subunit of K_{Ca} channel-knockout (β_1 ^{-/-}) mice (4) (22–30 g body wt) were used. Experiments were conducted according to the Helsinki Declaration and the “Guiding Principles in the Care and Use of Laboratory Animals” endorsed by the American Physiological Society. All animal protocols were approved by the Animal Care and Use Committee of the University of Virginia. All animals were genotyped after the experiment.

Mouse Cremaster Preparation

Mice were anesthetized with pentobarbital sodium (Nembutal; 40 mg/kg ip, diluted in isotonic saline to 5 mg/ml) and placed on a Plexiglas board. Body temperature was maintained at 35–36°C with a heating pad throughout the surgery and the experiment. The right cremaster muscle was exposed and opened by a longitudinal incision on its ventral surface. The testis and epididymis were excised after ligation of the supply vessels, and the cremaster muscle was pinned out on a silicone rubber pedestal. The mouse was placed on the stage of an Olympus microscope (BX 50 WI, Gibraltar Platform), and the cremaster muscle was continuously superfused at 3 ml/min with a bicarbonate-buffered saline solution (mM: 131.9 NaCl, 4.7 KCl, 2.0 CaCl₂, 1.2 MgSO₄, and 20.0 NaHCO₃) kept at 35°C and equilibrated with 95% N₂-5% CO₂. The preparation was allowed to stabilize for 45–60 min before initiation of the experiment. Supplemental doses of dilute pentobarbital sodium anesthetic in isotonic saline (10 mg/kg ip) were administered as appropriate. At the end of the experiment, the animals were killed by an anesthetic overdose.

Vessel Diameters

The cremaster muscle was transilluminated, the microscope image was projected to a video camera (series 65, Dage-MTI), and the video output was displayed on a monitor (model HR1000, Dage-MTI). The inner diameter of the arterioles (27–67 μ m maximum diameter) was continuously measured using Diamtrak software (65).

Electrical Stimulation

A Ag-AgCl reference electrode immersed in the superfusate was positioned symmetrically around the cremaster muscle, and selected arterioles were stimulated (30 Hz, 2 ms, 30 V) for 10 s with triple-beveled micropipettes (3–4 μ m ID) filled with 1 M NaCl and connected to the cathode of a stimulator (model SD9, Grass Instrument). The location of the stimulating pipette was critical: it was inserted under the cremaster mesothelium and positioned directly above an arteriole at a distance selected to evoke a local constriction of ~50%.

Stimulation With Activators of Voltage-Dependent Na⁺ Channels

Arterioles were stimulated focally with a pressure-pulse ejection (500 ms, 10–15 psi) of the neurotoxins veratridine (100 μ M), α -pompilidotoxin (α -PMTX, 30 μ M), and ATX-II (10 μ M) using a micropipette (3–4 μ m ID), and the vasomotor response was evaluated at the application site. Activation of Na_v channels of the cremaster striated muscle causes constriction of these muscle fibers, which may interfere with the vasomotor response of the vessels. Therefore, the neurotoxins were applied to a selected arteriolar segment that was not closely surrounded (<20 μ m) by striated muscle.

Blood Pressure Measurement

Ten- to 14-wk-old mice were placed in a dark environment, and blood pressure and heart rate were determined in “blinded” fashion using a computerized tail-cuff system (Visitech Systems, Cary, NC). The animals were exposed to the measurement procedure for 7 days

before initiation of data recording, and typically three replicate blood pressure measurement sets were averaged over the course of several days. Reported means are the averages for multiples days.

Immunocytochemical Analysis

Anesthetized mice were perfused through the left ventricle with a warmed MOPS-buffered physiological saline solution (PSS) containing 1% fetal calf serum, 10 U/ μ l heparin, 10 μ M ACh, and 10 μ M sodium nitroprusside and then with 2% paraformaldehyde in MOPS-buffered PSS to fix the vasculature. The cremaster muscles were removed and postfixed overnight. The tissues were dehydrated, embedded in paraffin, sectioned (5 μ m), placed on charge-coated slides, and deparaffinized using standard procedures. For antigen retrieval, the slides were heated in a microwave oven in a citrate buffer. The sections were blocked with 0.5% BSA in PBS and incubated overnight at 4°C with a rabbit polyclonal primary antibody (1:250 dilution). Primary antibodies were directed against one of the seven specific isoforms of the Na⁺ channel (Na_v1.1, Na_v1.2, Na_v1.3, Na_v1.5, Na_v1.6, Na_v1.7, and Na_v1.9) or against all isoforms of the Na⁺ channel, i.e., pan-sodium antibodies (Upstate Biotechnology and Alomone Laboratories). Antibodies against the individual isoforms of Na_v channels were purchased from Alomone Laboratories; the Na_v1.9 channel-specific rabbit antibody obtained from Chemicon International, which yielded results very similar to those obtained with the antibody purchased from Alomone Laboratories, was also used. Binding of the primary antibody was analyzed by immunofluorescence and immunohistochemistry. For immunofluorescence, the sections were incubated with an Alexa 568-labeled goat anti-rabbit secondary antibody (Molecular Probes) for 1 h at room temperature, and the fluorescent signal was examined with a confocal microscope (Fluoview, Olympus, New Hyde Park, NY). For immunohistochemistry, the primary antibody was labeled with a biotinylated secondary antibody (1 h at room temperature), and the endogenous peroxidase activity was blocked with 0.45% H₂O₂ in methanol (20 min). The sections were then incubated with Vectastain ABC reagent (Vector Laboratories) for 30 min and developed with 0.1% 3,3'-diaminobenzidine (Dakocytomation) and 0.023% H₂O₂ in the dark (5 min). The resultant immunostaining was observed with an Olympus BX 51 microscope and DP 70 camera. As controls, the primary antibodies were preabsorbed with their respective antigen or omitted entirely (secondary alone).

In some experiments, after the vasculature was fixed by perfusion with 2% paraformaldehyde, immunofluorescence was used to study intact cremaster arterioles and aortas. The cremaster muscle was spread and pinned on a Sylgard pedestal, and selected arterioles were perfused via micropipette with the primary and secondary antibodies to target the endothelial cells directly. Aortas were removed and cut into 3- to 4-mm segments, which were opened longitudinally for en face observation. Silicone rubber adhesive was used to secure the segment edges to a glass slide, and the tissue was permeabilized with 1% Triton X-100 in MOPS-buffered PSS. Incubation with the primary and secondary antibodies was the same as that described for arterioles.

Isolation of Aortic Endothelial Cells for PCR

The chest cavity of anesthetized mice was opened, and the thoracic aortas were removed, cleared of connective tissue, and filled with MOPS-buffered PSS containing 1 mg/ml collagenase VIII (Sigma-Aldrich) and 3.36 U/ml elastase (Sigma-Aldrich). The vessels were then incubated for 4 min at 37°C and pulled gently over a blunted, silicone rubber-filled 23-gauge hypodermic needle to dislodge the endothelial cells, which were collected in a microcentrifuge tube on ice and immediately pelleted at 10,000 g for 5 min for use in RT-PCR.

RT-PCR

RNA was isolated using the RNeasy-4 PCR kit (Ambion) and reverse transcribed using Superscript RT-PCR reagents (Invitrogen).

Platelet endothelial cell adhesion molecule (PECAM) and desmin were used to confirm the purity of the endothelial cell samples as specific markers for endothelial cell and smooth muscle, respectively. $Na_v1.6$ channels, PECAM, and desmin were detected using previously published primer sets (15, 35). For the $Na_v1.6$ channel, the sequences of the primer pair were 5'-CAT CTT TGA CTT TGT GGT GGT CAT-3' (sense) and 5'-CGG ATA ACT CGG AAT AGG GTT G-3' (antisense), and the thermal cycling conditions were 50°C for 2 min, 60°C for 20 min, 95°C for 5 min, and 60 cycles at 94°C for 15 s and 59°C for 60 s with an extension at 72°C for 7 min (15, 35). The sequences of the primer pair were 5'-AGG GGA CCA GCA GCA CAT TAG G-3' (sense) and 5'-AGG CCG CTT CTC TTG ACC ACT T-3' (antisense) for PECAM (15, 35) and 5'-GCT CTC CCG TGT TCC CTC GAG CAG G-3' (sense) and 5'-GGC GAA GCG GTC ATT GAG CTC TTG C-3' (antisense) for desmin (15, 35), and the cycling conditions were 45°C for 30 min, 95°C for 2 min, and 35 cycles of 94°C for 15 s, 55°C for 30 s, and 72°C for 30 s with an extension at 72°C for 5 min.

Experimental Protocols

The changes in diameter were measured first at the stimulation site (local) and then 500, 1,000, and 2,000 μm upstream (Fig. 1A) in response to four separate stimuli. Maximal diameter was estimated during superfusion of 1 mM adenosine. Variations in diameter are expressed as percentage of the maximum possible constriction or dilation.

Damage of the endothelium. Selective endothelial cell damage was produced by injection of an air bubble via a side branch of the stimulated arteriole. A side branch was selected $\sim 1,000 \mu\text{m}$ upstream from the site of electrical stimulation. The side branch was cannulated with a micropipette (3–4 μm ID), and a bolus of air was injected. After 45–60 min of recovery, the endothelial damage was evaluated by focal application via pressure-pulse ejection of 10 μM ACh (700 ms, 15–20 psi; Fig. 1A) from a micropipette (3–4 μm ID) at locations previously examined during responses to electrical stimulation (i.e., local and 500, 1,000, 1,500, and 2,000 μm upstream), and the change in diameter was analyzed only at the ACh application site. The localized reduction in the response to ACh (see

RESULTS) provided evidence that the endothelial cell damage caused by the air bubble was restricted to a short vessel segment that typically was closely surrounded by striated muscle. The close association between vessel and striated muscle in many cases precluded selective stimulation of the vessel with activators of Na_v channels because of simultaneous activation of striated muscle cells (see *Stimulation With Activators of Na_v*). Therefore, to assess participation of the endothelial cells in the response to Na_v channel activators in an arteriolar segment not closely surrounded by striated muscle, we disrupted the endothelium along the entire vessel length by perfusing 0.01% saponin (~ 20 s) via micropipette ($\sim 10 \mu\text{m}$ ID) through a side branch. In these experiments, the endothelial cell function was also analyzed by focal stimulation with a pulse of ACh.

Buffering of endothelial cell Ca^{2+} . A side branch of the selected arteriole $>2,000 \mu\text{m}$ upstream from the local site (Fig. 1A) was cannulated with a micropipette ($\sim 10 \mu\text{m}$ ID) and perfused with 10 μM BAPTA-AM for ~ 10 min to buffer the endothelial cell Ca^{2+} (67). Subsequent vasomotor responses to electrical stimulation were analyzed 30–40 min after perfusion and restoration of blood flow. BAPTA-AM was prepared in MOPS-buffered saline solution containing 1% low-endotoxin BSA. Chelation of endothelial cell Ca^{2+} was confirmed by demonstration of blockade of the vascular response to ACh delivered from a micropipette filled with a 10 μM ACh solution.

Focal application of Ni^{2+} , charybdotoxin, or nifedipine. The tip ($\sim 10 \mu\text{m}$ ID) of a micropipette filled with MOPS-buffered saline solution containing 100 μM Ni^{2+} , 1 μM charybdotoxin (ChTX), or 10 μM nifedipine was positioned above the arteriole, and the blockers were ejected by pressure over a 5- to 10-min period for Ni^{2+} or a 10- to 15-min period for ChTX or nifedipine. Nifedipine was superfused at the electrical stimulation site (local), and Ni^{2+} or ChTX was applied 1,000 μm upstream (Fig. 1A).

Topical application of drugs. The responses were assessed under control conditions and during topical application of the selected drug. A K^+ channel blocker, 1 μM TTX, 0.5 mM bupivacaine, 10 μM Ni^{2+} , 100 μM amiloride, or 100 nM prazosin, was applied for 15 min and 100 μM N^G -nitro-L-arginine (L-NNA) for 45 min. K^+ channel blockers included glibenclamide (1 μM), $BaCl_2$ (50 μM), and tetraethylammonium (TEA, 1–10 mM), which were used to block ATP-sensitive K^+ , inward rectifier K^+ , and K_{Ca} channels, respectively.

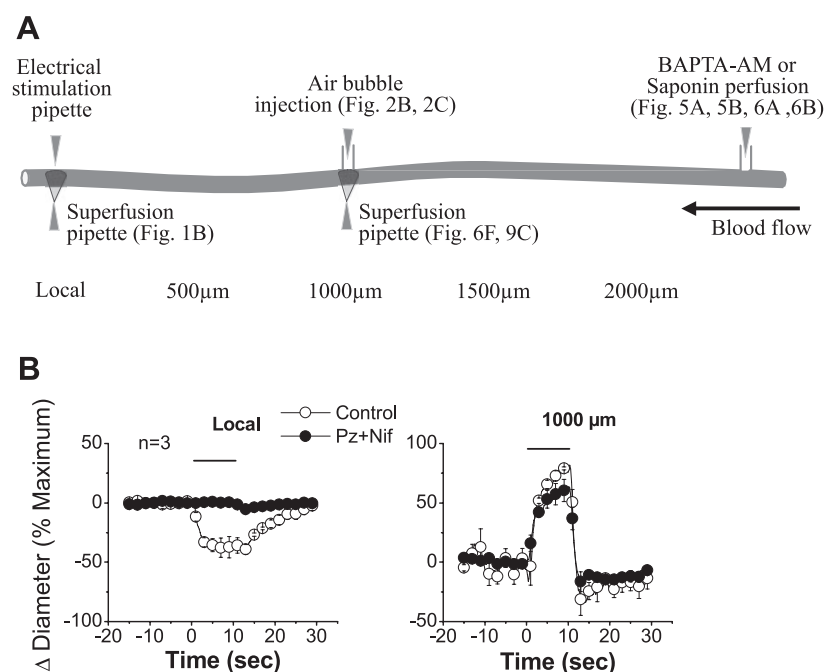


Fig. 1. A: schematic representation of experimental procedures. Local, 500 μm , 1,000 μm , and 2,000 μm denote sites at which vasomotor responses were assessed. References to other figures indicate locations of the suffusion pipette when the indicated data were obtained. B: local vasoconstriction at the stimulation site is not required for induction of electrically induced conducted vasodilation. The α -adrenoceptor antagonist prazosin (Pz, 100 nM) was applied topically in combination with focal superfusion via micropipette of 10 μM nifedipine (Nif) to block the neural component of response to electrical stimulation and direct activation of L-type, voltage-dependent Ca^{2+} channels, respectively. Response to electrical stimulation was evaluated at the stimulation site (local) and 1,000 μm upstream from the stimulation site. Values are means \pm SE. Horizontal bars indicate stimulation period.

Chemicals

TTX, glibenclamide, BaCl₂, TEA, veratridine, prazosin, nifedipine, and chemicals of analytic grade were purchased from Sigma Chemical (St. Louis, MO). L-NNA and ChTX were obtained from Research Biochemicals International (Natick, MA), BAPTA-AM from Molecular Probes (Eugene, OR), bupivacaine and pentobarbital sodium from Abbott Laboratories (North Chicago, IL), and BSA from United States Biochemical (Cleveland, OH). The toxins α -PMTX and ATX-II were purchased from Alomone Laboratories.

Statistical Analysis

Values are means \pm SE. Comparisons between groups were made using paired or unpaired Student's *t*-test, one-way ANOVA plus Newman-Keuls post hoc test, or two-way ANOVA as appropriate. *P* < 0.05 was considered significant.

RESULTS

Manipulation of tissue associated with the preparation of *in vitro* specimens can produce fundamental alterations in the patterns of cell-cell communication in the vessel wall (62); therefore, the present work was confined to the study of conduction of vasodilation in arterioles of the intact mouse cremaster muscle preparation (20). The cremaster arterioles manifest conducted vasomotor stimuli that propagate >2 mm without decay in response to ACh (data not shown) or electrical stimulation (20). For the experiments reported here, we selected electrical stimulation, because the response to this stimulus does not depend on activation of a receptor and, thus, could be defined more specifically in terms of the mechanisms involved in the conduction of the vasomotor responses. As described previously (20), electrical stimulation evoked a local vasoconstriction, presumably due to electrical activation of the smooth muscle cells. At the same time, a conducted vasodilation originates in the vessel on either side of the constriction and spreads along the entire arteriole without decay, suggesting that a regenerative mechanism of some type was triggered by the electrical stimulation (see Figs. 1, 2, 5, 7, and 8).

Vasodilator Signal Does Not Depend on Smooth Muscle Stimulation

It could be hypothesized that electrical stimulation opens smooth muscle L-type Ca²⁺ channels, leading to diffusion of Ca²⁺ from the activated smooth muscle cells to endothelial cells via myoendothelial gap junctions (6, 13, 67), with secondary triggering of a delayed, endothelium-dependent vasodilator response (67). Two observations indicate that this was not the case, however: 1) the local and conducted responses to electrical stimulation occurred with no detectable delay between them (see Figs. 1, 2, 5, 7, and 8), and 2) the elimination of the local vasoconstriction and, presumably, the rise in smooth muscle Ca²⁺ with a combination of the α -adrenoceptor antagonist prazosin (100 nmol/l) and focal superfusion via micropipette of 10 μ M nifedipine (Fig. 1A) did not affect the electrically induced conducted vasodilation (Fig. 1B). This observation also excludes mechanical distortion of the vessel wall or a hemodynamic effect at the site of constriction as triggers for the propagation and supports the hypothesis that electrical stimulation directly activates the endothelial cells, as has been recently proposed (20).

Endothelium Is Required for Propagation of the Vasodilator Signal

To assess the cellular pathway followed by the electrically induced vasodilator signal, we damaged the endothelium by injecting an air bubble via a side branch \sim 1,000 μ m upstream from the stimulus (Fig. 1A). After injection of the air bubble, endothelial cell function was reevaluated at locations surrounding the injection site by focal application of 10 μ M ACh, an endothelium-dependent vasodilator. The air bubble caused a decrease in baseline diameter (Table 1), and a selective reduction in reactivity to ACh in the region surrounding the site of injection (Fig. 2A). Although the disruption of the endothelium was restricted to the air bubble injection area (Fig. 2A), the air bubble-induced damage eliminated the regenerative component of the conducted dilation, leaving in its place a decremental conduction with a length constant of slightly more than 1 mm (Fig. 2B), a finding consistent with the previously demonstrated Cx40 sensitivity of the electrically induced conducted response and with the endothelial cell localization of Cx40 (20). These data indicate that integrity of the endothelium is essential for the nondecremental propagation of the electrically induced vasodilator signal.

Na_v Channel Is Involved in Generation of the Regenerative Response

We hypothesized that the conducted vasodilator signal reflected activation of a regenerative electrical signal at the stimulation site, which would involve one or more voltage-sensitive ion channels, such as Na_v and Ca_v. Although not widely appreciated, expression of the Na_v channel has been repeatedly detected in endothelial cells (25, 26, 55, 58), and TTX attenuates the propagation of the vasodilator response (Fig. 2C). However, the effect of TTX was modest, perhaps indicating the involvement of a TTX-resistant Na_v channel. We, therefore, applied the local anesthetic bupivacaine, which blocks TTX-sensitive and TTX-resistant Na_v channels (46) and found that it abolished the regenerative component of the

Table 1. Effect of experimental maneuvers on resting arteriolar diameter

Treatment	n	Arteriolar Diameter, μ m	
		Before	After
TTX (1 μ M)	6	26.8 \pm 2.1	24.5 \pm 2.9
Bupivacaine (500 μ M)	6	29.5 \pm 3.9	26.4 \pm 4.0*
Saponin (0.01%)	4	28.7 \pm 4.6	27.6 \pm 4.2
Endothelial damage	4	35.1 \pm 4.4	29.5 \pm 3.9*
BAPTA-AM perfusion	5	21.5 \pm 1.5	23.7 \pm 2.1
Amiloride (100 μ M)	4	27.7 \pm 4.4	22.0 \pm 3.1*
L-NNA (100 μ M)	4	28.1 \pm 2.5	24.6 \pm 2.5*
Ba ²⁺ (50 μ M)	3	29.9 \pm 3.0	24.1 \pm 3.6*
Glibenclamide (1 μ M)	3	22.3 \pm 2.8	15.3 \pm 3.1*
TEA			
1 mM	4	27.6 \pm 3.4	24.1 \pm 2.2*
10 mM	5	29.0 \pm 3.0	25.3 \pm 2.3*

Values are means \pm SE. Endothelium was damaged by perfusion of saponin or injection of an air bubble through a side-branch \sim 1,000 μ m upstream from the local site. BAPTA-AM (10 μ M) was perfused for \sim 10 min via a side branch. TTX, bupivacaine, amiloride, N^G-nitro-L-arginine (L-NNA), Ba²⁺, glibenclamide, and tetraethylammonium (TEA) were applied topically. **P* < 0.05 vs. Before (by paired Student's *t*-test).

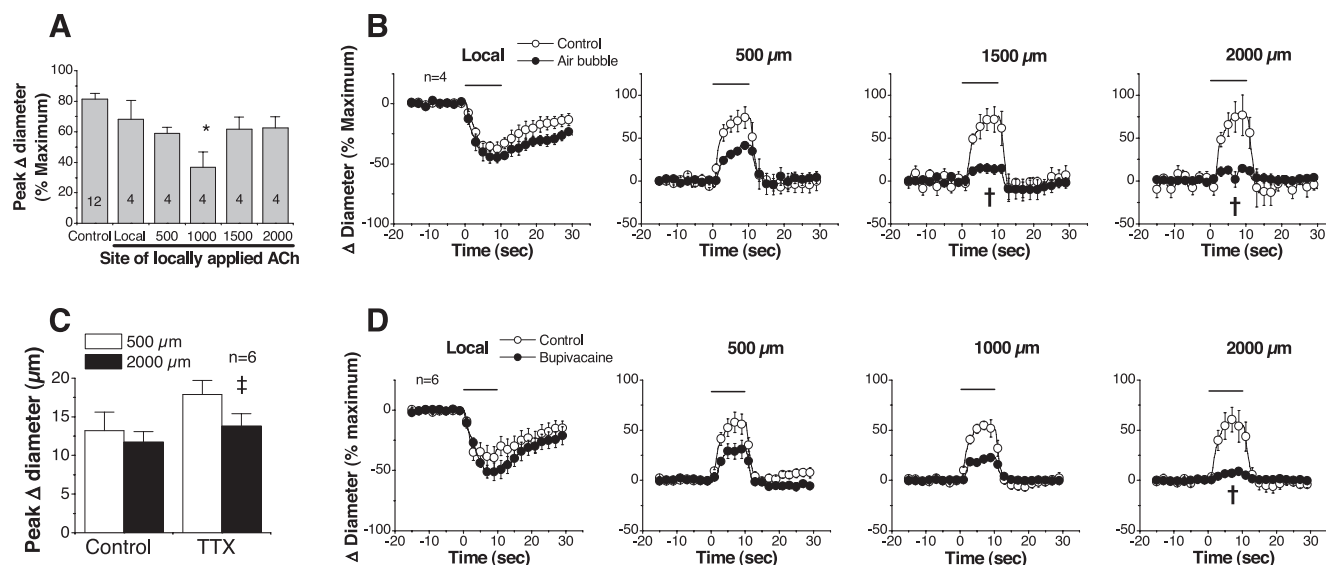


Fig. 2. Vasodilator signals spread via the endothelium and depend on voltage-dependent Na^+ channel activation. **A**: response to focal application of $10 \mu\text{M}$ ACh after air bubble damage compared with untreated (control) arterioles. Air bubble was injected via a side branch $\sim 1,000 \mu\text{m}$ upstream from the electrical stimulation site (local). ACh was applied at locations previously examined during responses to electrical stimulation (i.e., local and 500, 1,000, 1,500, and 2,000 μm upstream). In each case, response to ACh was analyzed at the site of application. Numbers within bars represent n . **B**: time course of electrically induced conducted vasodilation in control conditions and after injection of an air bubble into the endothelium. **C**: peak response of electrically induced vasodilation in control conditions and in the presence of $1 \mu\text{M}$ TTX. **D**: time course of electrically induced conducted vasodilation in the absence (control) and presence of $500 \mu\text{M}$ bupivacaine. Response to electrical stimulation was evaluated at the stimulation site (local) and 500, 1,000, and 2,000 μm upstream from the site (**B** and **D**) or only at the conducted sites [500 and 2,000 μm] (**C**). Values are means \pm SE. Horizontal bars indicate stimulation period. * $P < 0.05$ vs. control (by 1-way ANOVA plus Newman-Keuls post hoc test). † $P < 0.05$ vs. 500 μm (by one-way ANOVA plus Newman-Keuls post hoc test). ‡ $P < 0.05$ vs. 500 μm (by paired Student's t -test).

conducted response without affecting the magnitude of the local response (Fig. 2D). The magnitude of the residual dilation during the application of bupivacaine decayed rapidly along the vessel, as expected for passive, electrotonic spread of an electrical signal.

These findings suggest that the endothelium-dependent, non-decremental vasodilator signal relies on the regenerative activation of the Na_v channel along the vessel length. Given the novelty of this proposition, we screened for endothelial cell expression of the Na_v channel by immunocytochemistry using a battery of 10 antibodies: 2 were directed against all known isoforms of the Na_v channel (pan- Na_v antibodies), and 8 were targeted to specific isoforms of these channels ($\text{Na}_v1.1$, $\text{Na}_v1.2$, $\text{Na}_v1.3$, $\text{Na}_v1.5$, $\text{Na}_v1.6$, $\text{Na}_v1.7$, and $\text{Na}_v1.9$ antibodies). The pan- Na_v antibodies reacted with endothelium and smooth muscle of cremaster arterioles (data not shown), and, in whole-mount arterioles perfused with the primary and secondary antibodies, the signal for the Na_v channel was mainly detected at borders of the endothelial cells (data not shown). Isoform-specific antibodies for $\text{Na}_v1.2$, $\text{Na}_v1.6$, and $\text{Na}_v1.9$ channels also labeled the arterioles. The $\text{Na}_v1.2$ channel was mainly detected in the endothelial cells, whereas $\text{Na}_v1.6$ and $\text{Na}_v1.9$ channels were present in both cells of the vessel wall (Fig. 3, A–F). Antibodies preabsorbed with their respective antigen did not yield a fluorescent signal (Fig. 3, D–I).

PCR screen for message in the arteriolar endothelium would have been desirable, but it was not practical to obtain sufficiently pure endothelial cell samples from arterioles. We, therefore, examined endothelium from the mouse aorta as a surrogate and were able to detect the $\text{Na}_v1.6$ channel by immunofluorescence (Fig. 3J), as well as the message for this channel in freshly isolated endothelial cells by RT-PCR (Fig.

3K). These data support the idea that the endothelium may normally express Na_v channels and, thus, the immunocytochemical analysis of the arterioles.

The presence of TTX-resistant ($\text{Na}_v1.9$) and TTX-sensitive ($\text{Na}_v1.2$ and $\text{Na}_v1.6$) Na_v channels in the endothelial cells suggests a second possibility to explain the modest sensitivity of the conduction process to TTX compared with bupivacaine. Arteriolar endothelium manifests a very low permeability to hydrophilic solutes (34), and a water-soluble drug such as TTX, when topically applied, might have limited access to luminal sites or to some tight junction-associated microdomain of the endothelial cells, whereas a lipid-soluble agent (45) such as bupivacaine might reach the Na_v channels. To assess this possibility, we turned to three specific activators of the Na_v channel: the well-defined, lipid-soluble neurotoxin veratridine and two water-soluble polypeptide neurotoxins, α -PMTX and ATX-II (*Anemonia sulcata* toxin) (9, 59). Stimulation with a pulse of veratridine evoked a large, rapid vasodilation (Fig. 4A). In contrast, α -PMTX and ATX-II induced more modest and transient vasoconstrictions (Fig. 4C). The finding that luminal application of saponin (Fig. 1A) converted the large veratridine-activated vasodilation to a vasoconstriction (Fig. 4A) similar to that induced by the water-soluble neurotoxins α -PMTX and ATX-II (Fig. 4C) further supports the involvement of an endothelial Na_v channel in the vasodilator response to veratridine (Fig. 4A). Saponin perfusion also impaired the response to ACh (Fig. 4B), corroborating the disruption of the endothelium. In addition, the veratridine response was resistant to TTX and sensitive to bupivacaine, as was observed with electrical stimulation (Fig. 4D). All these findings support the idea that access to endothelial Na_v channels is limited for water-soluble neurotoxins (TTX, α -PMTX,

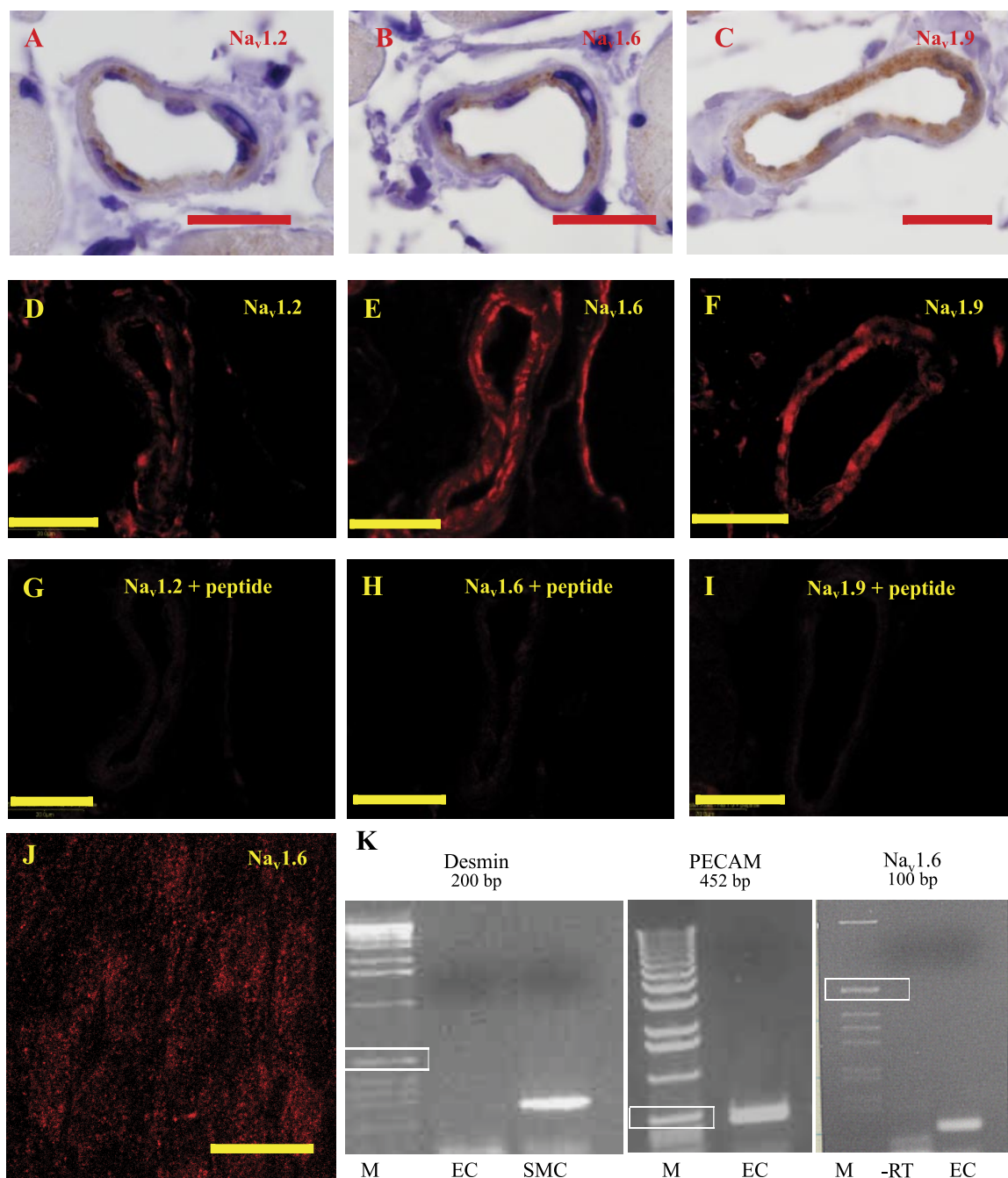


Fig. 3. Voltage-dependent Na^+ (Na_v) channel expression in mouse endothelial cells. *A–C*: immunohistochemical detection of expression of Na_v channel-specific isoforms $\text{Na}_v1.2$, $\text{Na}_v1.6$, and $\text{Na}_v1.9$ in endothelial cells of cremaster arterioles. *D–I*: immunofluorescence of $\text{Na}_v1.2$, $\text{Na}_v1.6$, and $\text{Na}_v1.9$ channels in serial sections of cremaster muscle incubated with primary antibodies in control conditions (*D–F*) or preabsorbed with their appropriate peptide antigen (*G–I*). *J*: immunocytochemistry for $\text{Na}_v1.6$ channel in aortic endothelium. Scale bars, 20 μm . *K*: RT-PCR for desmin, platelet endothelial cell adhesion molecule (PECAM), and $\text{Na}_v1.6$ channel in freshly isolated aortic endothelial cells. In different gels prepared with the same endothelial cell sample, mRNA for endothelial cell (EC) and smooth muscle cell (SMC) markers PECAM and desmin was assayed. Positive reaction for PECAM and negative reaction for desmin corroborate selectivity of endothelial cell isolation. RT-PCR confirms $\text{Na}_v1.6$ channel mRNA expression in these cells. –RT, omission of reverse transcriptase to rule out direct amplification of DNA. Lane M, DNA size standards; white boxes, position of 500 bp.

and ATX-II) and that only lipid-soluble drugs (veratridine and bupivacaine) can reach these channels.

Endothelial Cell Ca^{2+} Mediates Vasodilation but not Conduction

How might an Na_v channel-dependent propagating depolarization lead to dilation? Endothelial cell-mediated dilata-

tion typically involves Ca^{2+} as a second messenger; accordingly, to test for a role of endothelial cell cytoplasmic Ca^{2+} in the conducted vasodilator response, we buffered endothelial cell Ca^{2+} by perfusing the arterioles for 10 min with 10 μM BAPTA-AM via a side branch located upstream from the 1,000 μm -site (Fig. 1A). BAPTA-AM perfusion did not alter baseline diameter (Table 1) but markedly

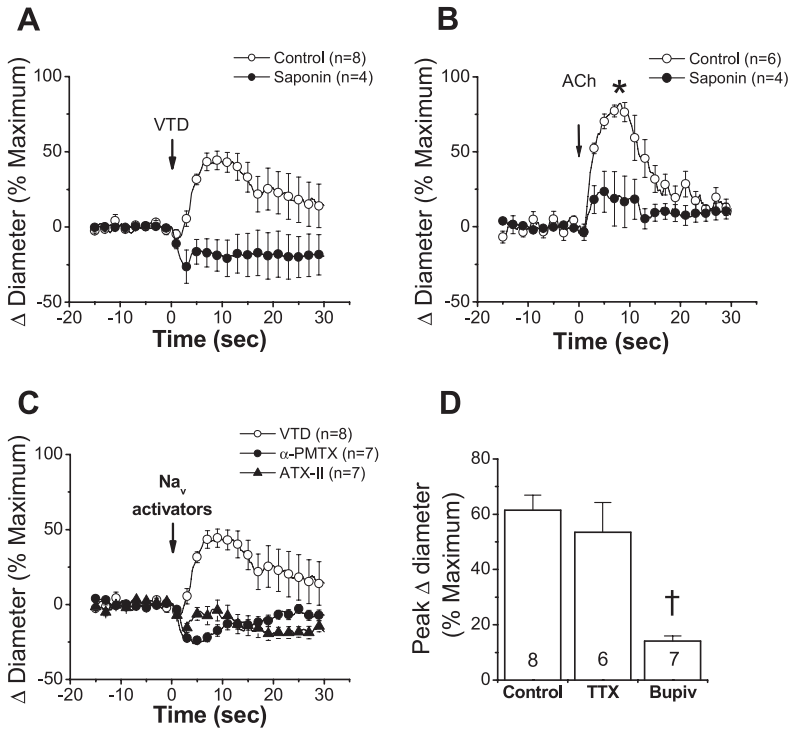


Fig. 4. Vasomotor response induced by lipid- and water-soluble activators of Na_v channels. *A*: time course of the vasomotor response induced by the lipid-soluble neurotoxin veratridine (100 μ M, VTD) in control conditions and after disruption of the endothelium by perfusion of 0.01% saponin via a side branch upstream from the local site (see Fig. 1A). *B*: vasodilator response to focal application of 10 μ M ACh after saponin treatment compared with untreated (control) arterioles. *C*: comparison of veratridine-evoked vasodilation with vasoconstriction elicited by water-soluble neurotoxins α -pompilidotoxin (30 μ M, α -PMTX) and *Anemonia sulcata* toxin (10 μ M, ATX-II). *D*: vasodilator response to veratridine in the absence (control) or presence of 1 μ M TTX or 500 μ M bupivacaine (Bupiv). Numbers within bars represent *n*. Response to neurotoxins (VTD, α -PMTX, and ATX-II) and ACh was analyzed at the stimulation site. Values are means \pm SE. **P* < 0.05 vs. control (by 2-way ANOVA). †*P* < 0.05 vs. control (by 1-way ANOVA plus Newman-Keuls post hoc test).

altered the vasomotor response evoked by electrical stimulation, leading to enhanced and prolonged local vasoconstriction. In addition, endothelial cell BAPTA loading caused a conspicuous delay and a clear reduction of the conducted vasodilation (Fig. 5A). The increase in diameter

was also slower after BAPTA-AM perfusion. Furthermore, BAPTA unmasked a vasoconstrictor response to an ACh pulse (700 ms), confirming the endothelial cell Ca^{2+} buffering (Fig. 5B). We hypothesize that the dilation remaining after BAPTA loading reflects activation of a slow, Ca^{2+} -

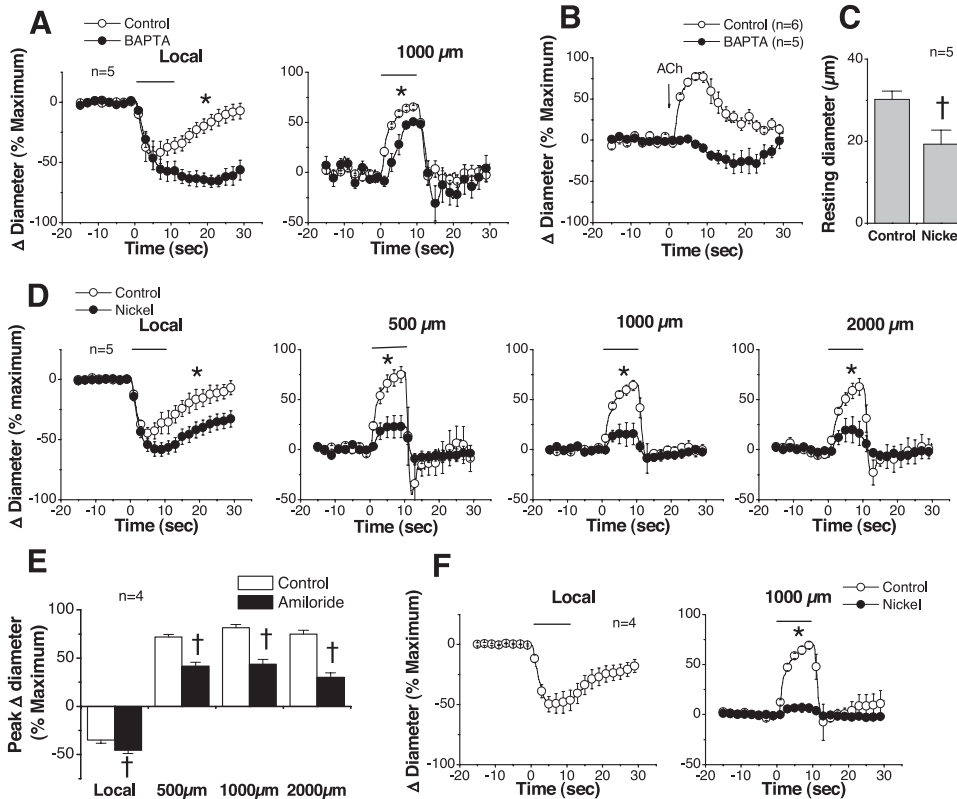


Fig. 5. Conducted vasodilation depends on activation of a Ca^{2+} -dependent signaling pathway. *A*: time course of vasomotor response to electrical stimulation before (control) and after endothelial cell Ca^{2+} was buffered with 10 μ M BAPTA-AM applied for \sim 10 min by intravascular microvessel perfusion via a side branch $>$ 2,000 μ m upstream from the stimulation site (local, see Fig. 1A). *B*: assessment of endothelial cell Ca^{2+} buffering by focal application of 10 μ M ACh. *C*: reduction in resting diameter evoked by topical application of 10 μ M Ni^{2+} . *D*: electrically induced conducted vasodilation in the absence (control) and presence of 10 μ M Ni^{2+} . *E*: peak response induced by electrical stimulation in control conditions and after topical application of 100 μ M amiloride. *F*: blockade of electrically induced conducted vasodilation by focal application via micropipette (Fig. 1A) of 100 μ M Ni^{2+} 1,000 μ m upstream from the local site. Response to electrical stimulation was evaluated at the local site and 500, 1,000, and 2,000 μ m upstream (*D* and *E*) or only at the local site and 1,000 μ m upstream (*A* and *F*). Values are means \pm SE. Horizontal bars indicate stimulation period. **P* < 0.05 vs. control (by 2-way ANOVA). †*P* < 0.05 vs. control (by paired Student's *t*-test).

independent vasodilator signal or saturation of the Ca^{2+} -chelating capacity of BAPTA during the stimulation period (10 s).

Activation of T-Type Ca^{2+} Channels

The foregoing results indicate that changes in endothelial cell Ca^{2+} are required for activation of the electrically induced conducted vasodilator response, which suggests that activation of the Na_v channel may be coupled to some voltage-sensitive Ca^{2+} signaling pathway, and Ca_v3 channels have been identified in endothelial cells (21, 57, 61, 63, 70). Of the three pore-forming subunits of Ca_v3 channels that are known [α_{1G} ($\alpha_{13.1}$), α_{1H} ($\alpha_{13.2}$), and α_{1I} ($\alpha_{13.3}$)], $\alpha_{13.1}$ and $\alpha_{13.2}$ have been detected in blood vessels (10, 28, 56, 63). Therefore, we explored the participation of Ca^{2+} channels in the response to electrical stimulation. We were unable to visualize the protein expression using immunocytochemistry, because good antibodies were absent, and recognizing the limitations of the available blockers, we tested three structurally different Ca_v3 channel antagonists: mibefradil, Ni^{2+} , and amiloride (33, 54, 68). Ni^{2+} and amiloride exhibit higher affinity for the $\text{Ca}_v3.2$ channel, whereas mibefradil is not a subtype-specific blocker (32, 33, 54, 68). Treatment with 1 μM mibefradil resulted in near-maximal vasodilation, which precluded further assessment of electrically induced conducted dilator responses (data not shown). We presume that the dilation arose as a result of well-known, nonspecific effects of mibefradil (29, 30, 36, 39, 43, 64).

In contrast to mibefradil, topical application of 10 μM Ni^{2+} or 100 μM amiloride caused vasoconstriction (Fig. 5C, Table 1) and enhanced the local vasoconstriction evoked by electrical stimulation (Fig. 5, D and E), as observed with BAPTA treatment. Both blockers of the Ca_v3 channel drastically reduced the magnitude of the conducted component of the electrically induced response. Although the conducted

dilation was reduced at each measurement site compared with control, the remaining dilator response was propagated along the vessel without decrement (Fig. 5, D and E).

The reduction in magnitude of the conducted vasomotor response caused by Ni^{2+} and amiloride (Fig. 5, D and E) could reflect the involvement of the Ca_v3 channel at either or both of two locations: 1) the site of stimulation, where the propagated vasodilator signal is initiated, or 2) the distant site, where the conducted electrical signal is transduced to a mechanical response. To distinguish between these two possibilities, we applied 100 μM Ni^{2+} focally via micropipette 1,000 μm upstream from the stimulation site (Fig. 1A). This treatment blocked the dilation at the site at which it was applied (Fig. 5F). Comparison of the vasomotor response in the setting of focal (Fig. 5F) and global (Fig. 5, D and E) Ca_v3 channel blockade suggests that opening of these Ca^{2+} channels mediates the coupling between activation of Na_v channels and the vasodilator response along the vessel length, but not the conduction process itself.

The Ni^{2+} and amiloride sensitivity of the response to electrical stimulation offers pharmacological evidence for involvement of the $\text{Ca}_v3.2$ channel in the conducted vasodilation. Therefore, the pharmacology was extended by examination of the behavior of $\alpha_{13.2}^{-/-}$ mice (10). In $\alpha_{13.2}^{-/-}$ mice, the conducted vasodilator response induced by electrical stimulation was severely attenuated, although the magnitude of the local vasoconstriction was similar to that observed in wild-type mice: -51.6 ± 4.3 and $-47.3 \pm 1.9\%$, respectively (Fig. 6A). As might be expected, 10 μM Ni^{2+} did not cause significant vasoconstriction in arterioles from $\alpha_{13.2}^{-/-}$ mice (Fig. 6B). Moreover, resting arteriolar tone and blood pressure were higher in knockout than in wild-type mice (Fig. 6, C and D), indicating that $\text{Ca}_v3.2$ channels play a role in the tonic control of peripheral resistance.

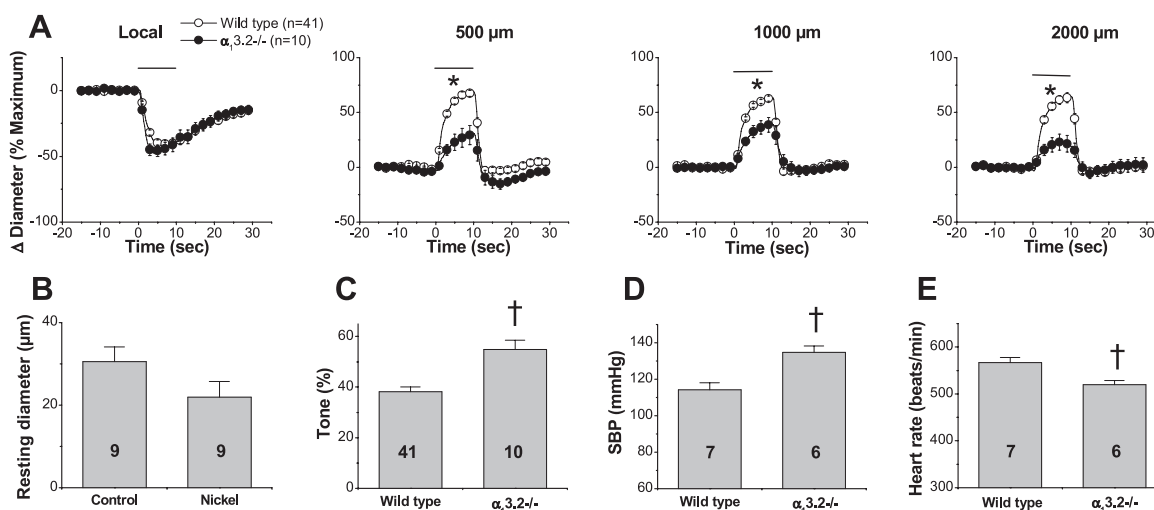


Fig. 6. $\text{Ca}_v3.2$ channel-knockout ($\alpha_{13.2}^{-/-}$) mice show an impaired conducted vasodilation and elevated blood pressure. **A**: time course of electrically induced conducted vasodilation in wild-type and $\alpha_{13.2}^{-/-}$ mice. Response to electrical stimulation was evaluated at the stimulation site (local) and 500, 1,000, and 2,000 μm upstream. **B**: effect of topical application of 10 μM Ni^{2+} on arteriolar resting diameter of $\alpha_{13.2}^{-/-}$ mice. **C**: spontaneous myogenic vasoconstrictor tone in wild-type and $\alpha_{13.2}^{-/-}$ mice expressed as percentage of maximum diameter. **D** and **E**: tail-cuff systolic blood pressure (SBP) and heart rate, respectively. Slower heart rate in $\alpha_{13.2}^{-/-}$ mice supports the idea that $\text{Ca}_v3.2$ channels participate in generation of pacemaker potential in the heart (69). Numbers within bars represent *n*. Values are means \pm SE. Horizontal bars represent stimulation period. **P* < 0.05 vs. wild-type (by 2-way ANOVA). [†]*P* < 0.05 vs. wild-type (by unpaired Student's *t*-test).

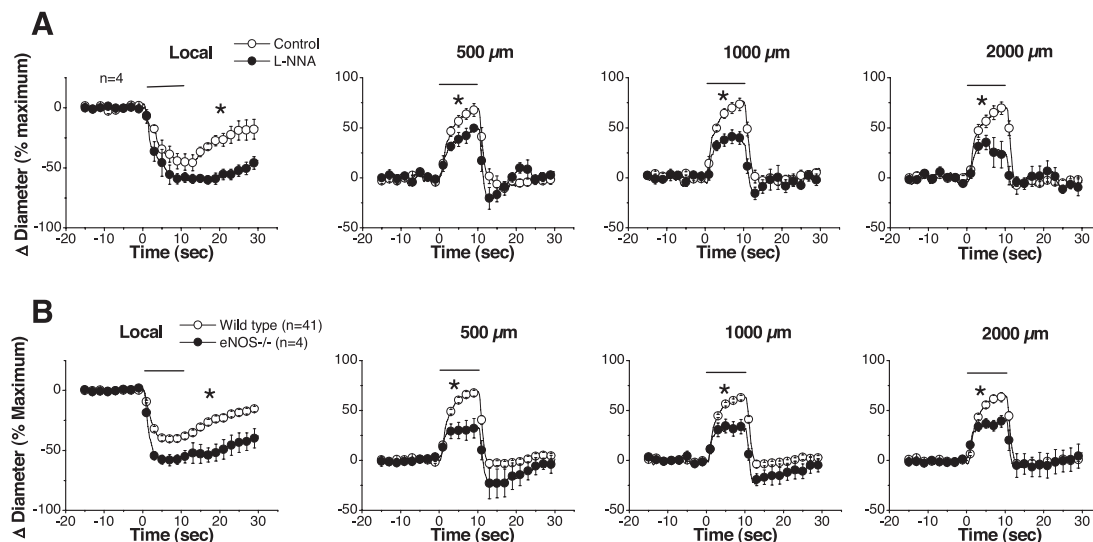


Fig. 7. Activation of endothelial nitric oxide synthase (eNOS) participates in electrically induced conducted vasodilation. *A*: time course of electrically induced conducted vasodilation in control conditions and after treatment with 100 μM *N*^G-nitro-L-arginine (L-NNA). *B*: conducted vasodilator response elicited by electrical stimulation in wild-type and eNOS^{-/-} mice. Response to electrical stimulation was evaluated at the stimulation site (local) and 500, 1,000, and 2,000 μm upstream. Values are means ± SE. Horizontal bars indicate stimulation period. **P* < 0.05 vs. control or wild-type (by 2-way ANOVA).

Activation of NO Production and K⁺ Channels

We hypothesize that an Na_v channel-mediated depolarization triggers influx of Ca²⁺ into the endothelial cells by opening Ca_v3.2 channels, thereby activating Ca²⁺-dependent, endothelium-mediated dilator mechanisms. NO is a critical endothelial cell Ca²⁺-dependent vasodilator, and we used the NO synthase (NOS) antagonist L-NNA and eNOS^{-/-} mice to assess the participation of NO in the response to electrical stimulation. As anticipated, topical application of 100 μM L-NNA caused a reduction of resting arteriolar diameter (Table 1). In addition, this treatment enhanced the local vasoconstriction and reduced the conducted vasodilation induced by electrical stimulation (Fig. 7*A*), indicating that the endothelial cell Ca²⁺ signal initiated by electrical stimulation leads to NO production. A similar reduction in eNOS^{-/-} mice (Fig. 7*B*) strongly supports an endothelial origin for the NO released.

Because NO itself does not evoke conducted responses (14) and because Ca²⁺ channels participate, it seems likely that the electrically induced, NO-dependent vasodilation represents Ca²⁺-mediated activation of eNOS along the vessel length.

Blockade of NO production reduced but did not abolish the electrically induced conducted vasodilation. We therefore tested the participation of K⁺ channels in this response. TEA (1–10 mM), Ba²⁺ (50 μM), and glibenclamide (1 μM) reduced baseline diameter (Table 1). TEA enhanced the local vasoconstriction and inhibited the conducted vasodilation in a concentration-dependent manner (Fig. 8*A*), suggesting that the K_{Ca} channel is involved in the response to electrical stimulation. Neither Ba²⁺ nor glibenclamide affected the electrically induced vasomotor responses (Fig. 8*B*). Furthermore, focal application via micropipette of the K_{Ca} channel blocker ChTX (1 μM) 1,000 μm upstream from the stimulation site inhibited the

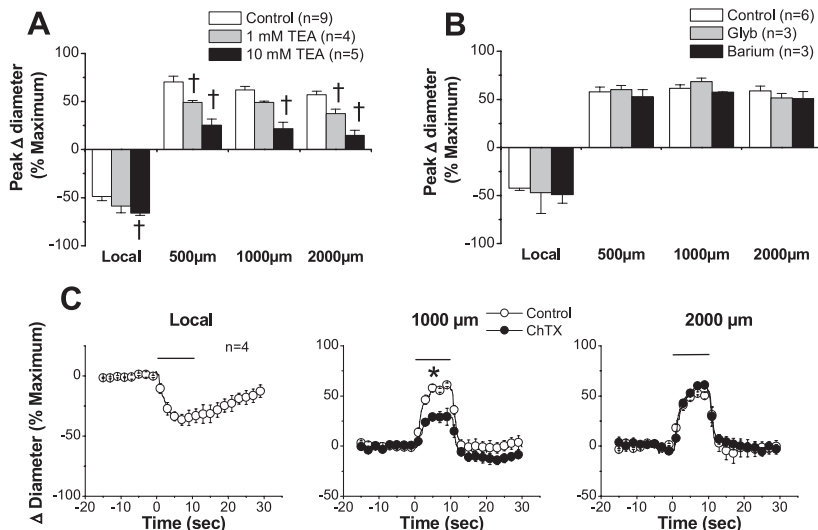


Fig. 8. Opening of Ca²⁺-activated K⁺ channels contributes to electrically induced conducted vasodilation. *A*: peak of vasomotor response to electrical stimulation in control conditions and during superfusion with 1–10 mM tetraethylammonium (TEA). *B*: peak of vasomotor response induced by electrical stimulation in control conditions and during superfusion with 1 μM glibenclamide (Glib) or 50 μM Ba²⁺. Because neither glibenclamide nor Ba²⁺ altered local vasoconstriction or conducted vasodilation, involvement of ATP-sensitive K⁺ channels or inward rectifier K⁺ channels in the response was excluded. *C*: focal application of 1 μM charybdotoxin (ChTX) at the conduction pathway (1,000 μm upstream from the local site; see Fig. 1*A*) of the electrically induced vasodilation. Local, 500 μm, 1,000 μm, and 2,000 μm denote stimulation (local) and conducted (500, 1,000, and 2,000 μm) sites, where response to electrical stimulation was evaluated. Values are means ± SE. Horizontal bars indicate stimulation period. **P* < 0.05 vs. control (by 2-way ANOVA). †*P* < 0.05 vs. control (by 1-way ANOVA plus Newman-Keuls post hoc test).

vasodilator response at the site of ChTX application but not the propagation of the electrically induced vasodilation to more distant vessel segments (Fig. 8C).

The activation of eNOS (Fig. 7) strongly supports the idea that the $Ca_v3.2$ channel-dependent conducted vasodilation was activated in the endothelial cells. However, we note that the $Ca_v3.2$ channels could be functionally coupled to a large-conductance K_{Ca} (BK_{Ca}) channel in the smooth muscle cells (10). It is known that the β_1 -subunit of the K_{Ca} channel is essential for effective coupling of Ca^{2+} to the BK_{Ca} channel in smooth muscle cells (4, 42); we therefore used $\beta_1^{-/-}$ mice (4) to evaluate the possible direct activation of smooth muscle BK_{Ca} channels by $Ca_v3.2$ channels. Deletion of the β_1 -subunit did not affect the electrically induced conducted vasodilation (Fig. 9), which further supports an endothelial origin for the $Ca_v3.2$ channel-dependent vasodilator signal.

DISCUSSION

Blood vessels are complex, multicellular structures in which cell and vessel functions must be coordinated. Functional coupling within the vascular network is manifested by conduction of vasomotor signals along the vessel length (27, 48, 49), and electrotonic spread of changes in membrane potential gives rise to many conducted vasomotor responses (27, 50, 62). It has also been observed that conduction may extend over longer distances than can be explained by passive electrotonic current spread (11, 12, 16, 20, 37); thus some active process must be invoked. Our results show that depolarizing electrical stimuli applied to a short arteriolar segment activate the vessel's contractile machinery at the site of stimulation, as would be expected (17, 20). In addition, activation of a nondecremental, nerve-independent conducted vasodilation propagates for remarkably long distances through the endothelium (Figs. 1 and 2). The behavior of this conducted response is not consistent with simple electrotonic conduction along the vessel axis; rather, the data argue that electrical activation of an endothelial Na_v channel initiates a depolarizing signal that spreads in a regenerative manner along the vessel length (Figs. 1–8). Furthermore, the propagating depolarization appears to be coupled to activation of $Ca_v3.2$ channel-dependent signaling pathways at distant sites (Figs. 5 and 6) that are responsible for the dilation. Among the Ca^{2+} -dependent pathways linking opening of the Ca^{2+} channel to dilation is activation of eNOS and the K_{Ca} channel (Figs. 7, 8, and 10). This linkage is indicated by the finding that damage of the endothelium or inhibition of the Na_v channel disrupted the regenerative component of the

electrically induced conducted vasodilation (Fig. 2), whereas blockade of $Ca_v3.2$ channels, eNOS, or the K_{Ca} channel reduced the magnitude of the conducted dilation without affecting the propagation of the response (Figs. 5–8).

Although the pharmacology implicating a role for Na_v channels is provocative, the uncertainty in specificity and access of the activators and inhibitors limits the interpretation of the data. The propositions advanced here must ultimately be tested with appropriate knockout animals and patch-clamp methods to define the electrical signature of the channels involved. This represents a serious technical challenge, however, since available data indicate that the microvessels are quite different from the conduit vessels, and our findings indicate that understanding this system will ultimately require investigation of intact microvessels in vivo.

The reduced magnitude of the conducted vasodilation observed after buffering the endothelial cell Ca^{2+} (Fig. 5), as well as the behavior of arterioles from eNOS-deficient mice (Fig. 7), supports the idea that there is coupling between $Ca_v3.2$ channels and Ca^{2+} -dependent endothelial cell function in this response. However, in our experiments, the K_{Ca} channel may have been activated indirectly in the smooth muscle cells, rather than in the endothelial cells by an NO-independent mediator such as the endothelium-derived hyperpolarizing factor (EDHF) (22, 51). The indirect activation of the K_{Ca} channel by an EDHF would be further supported by the reported lack of functional myoendothelial gap junctions in cremaster microvessels (52), and this possibility demands further exploration, including more detailed channel analysis in microvessels with selective study of smooth muscle and endothelial cells singly and in situ (31).

Although our data strongly support an endothelial origin of the $Ca_v3.2$ channel-dependent conducted vasodilation, it is in principle possible that the Ca^{2+} channel-dependent response was triggered in the smooth muscle cells. Recently, Chen et al. (10) proposed that the vasodilator response to ACh in the coronary artery relies on $Ca_v3.2$ channels functionally coupled to BK_{Ca} channels in the smooth muscle cells. However, this possibility is unlikely in our system, inasmuch as we found that the electrically induced conducted vasodilation is not altered in animals in which the β_1 -subunit of the K_{Ca} channel has been deleted (4) (Fig. 9). Although this subunit plays a critical role in the coupling of Ca^{2+} to the BK_{Ca} channel in smooth muscle cells (4, 42), it does not seem to be required for the direct activation of this channel by NO (1) or another endothelium-derived relaxing factor such as EDHF (8).

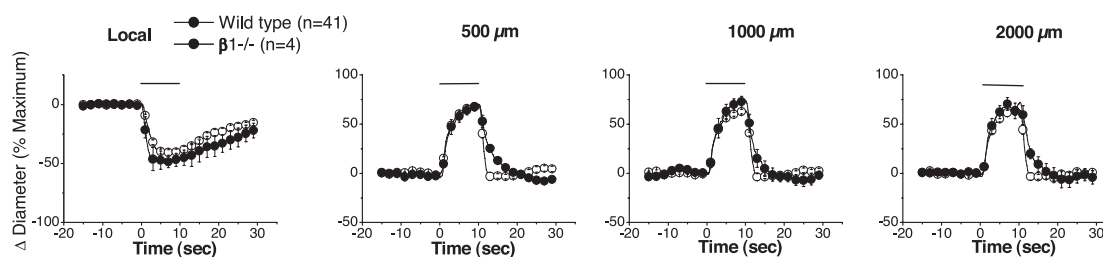


Fig. 9. $Ca_v3.2$ channels do not activate large-conductance Ca^{2+} -activated K^+ (BK_{Ca}) channels directly in smooth muscle cells. Time course of electrically induced conducted vasodilation in wild-type and β_1 -subunit-knockout ($\beta_1^{-/-}$) mice is shown. Response to electrical stimulation was evaluated at the stimulation site (local) and 500, 1,000, and 2,000 μm upstream. The β_1 -subunit of the BK_{Ca} channel is essential for BK_{Ca} channel activation by Ca^{2+} and is only expressed in smooth muscle cells (4, 41, 42). Deletion of the β_1 -subunit did not change the vasomotor response induced by electrical stimulation, arguing against a direct functional coupling between $Ca_v3.2$ and BK_{Ca} channels in smooth muscle cells. Values are means \pm SE. Horizontal bars indicate stimulation period.

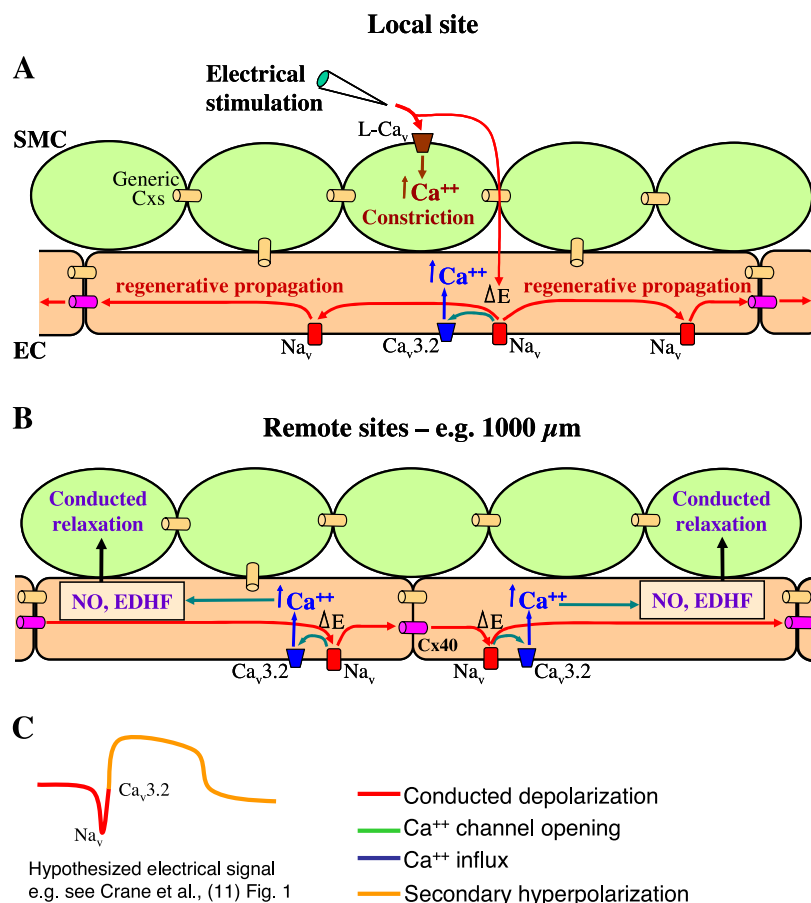


Fig. 10. Proposed interactions between Na_v channels and initiation of the conducted vasodilator response by $\text{Ca}_v3.2$ channels. Direct activation of L-type voltage-dependent Ca^{2+} channels by electrical stimulation results in a vasoconstriction at the stimulation site (local, A). In addition, electrical stimulation is hypothesized to trigger regenerative activation of endothelial Na_v channels (A), which results in a depolarizing signal (ΔE) that rapidly propagates along the endothelium (red line, A and B) via connexin 40 (Cx40) gap junctions (20). Conducted electrical signal is transduced into vasodilation by activation of $\text{Ca}_v3.2$ channels. Resultant endothelial cell (EC) Ca^{2+} influx triggers Ca^{2+} -sensitive vasodilator signals, which induce relaxation of the underlying smooth muscle cells (SMC, B). Activation of eNOS and endothelium-derived hyperpolarizing factor (EDHF) is shown, but others are likely to be involved. Secondary hyperpolarizing component (orange line) can persist long after passage of the depolarizing signal (C), because termination of the response will depend on the pattern of restoration of endothelial cell Ca^{2+} . There is good evidence that gap junctions link the cells of the vessel wall, providing electrical continuity and pathways for second-messenger signaling (18, 19, 27, 50). Decremental conduction that remains after deletion of Cx40 (20) indicates the presence of other connexins linking the vascular cells; for clarity and simplicity, these connexins are designated generic Cxs.

Deletion of $\text{Ca}_v3.2$ channels caused an increase in arteriolar vasomotor tone and blood pressure (Fig. 6), observations that highlight the critical importance of conducted vasomotor responses and the likely involvement of $\text{Ca}_v3.2$ channels in the tonic control of peripheral resistance. The conducted vasodilation was not eliminated in $\alpha_13.2^{-/-}$ mice, although it was eliminated with a high concentration of Ni^{2+} (Fig. 5F), which nonselectively blocks Ca_v3 channels. This might suggest that other channels, such as $\text{Ca}_v3.1$, which have been detected in the endothelium (61, 63, 70), are also involved in the vasodilator response. Interestingly, it has been observed that in myoblasts from $\alpha_13.2^{-/-}$ mice there is compensation of function by upregulation of $\text{Ca}_v3.1$ channels (10), which may have also occurred in the endothelial cells of the cremaster arterioles, masking the effect of the deletion of $\text{Ca}_v3.2$ channels.

To summarize, we report here several lines of evidence that support the conclusion that there is a rapid, conducted vasodilator signal that propagates along the endothelium over thousands of micrometers and that the propagation is not blocked by any of several K^+ or Ca^{2+} channel blockers. We present pharmacological evidence for the involvement of one or more Na_v channel isoforms in electrically induced dilations of arterioles. Furthermore, we advance the interpretation of the data that activation of the Na_v channel leads to a regenerative, depolarizing current that propagates along the vessel axis through the endothelium. The data support the proposition that the spreading depolarization is function-

ally coupled to eNOS and the K_{Ca} channel via activation of $\text{Ca}_v3.2$ channels. We note that an agonist such as ACh can likely trigger the same mechanism, since ACh-induced Ca^{2+} entry in freshly isolated endothelial cells is sensitive to membrane potential in a manner that cannot be simply explained by changes in the electrical driving force for Ca^{2+} (60). In addition, after buffering the endothelial cell Ca^{2+} with BAPTA, ACh evokes membrane depolarization (40) and an endothelium-dependent vasoconstriction (Figs. 2A, 4B, and 5B). Moreover, the response to electrical stimulation (Fig. 7) and the ACh-induced conducted vasodilation are coupled to Ca^{2+} -dependent NO production (5).

Our data are thus consistent with the discovery of a novel, vasodilator mechanism that relies on interplay between two voltage-sensitive ion channels in the endothelium (Fig. 10). Expression of functional voltage-dependent ion channels in the endothelial cells has enormous implications for cardiovascular homeostasis and offers new opportunities for understanding the key role of the endothelium in vascular function. These findings make it imperative that a greater understanding of the subtype distribution and function of vascular Na_v and Ca_v3 channels be developed, inasmuch as this pathway is likely to play an essential role in the tonic, endothelial control of arterial blood pressure, which may provide clues to the design of new therapeutic strategies for the treatment of cardiovascular diseases such as hypertension.

ACKNOWLEDGMENTS

We thank Dr. Victor E. Laubach for generously supplying the eNOS^{-/-} mice and Dr. Richard W. Aldrich for sharing the β_1 -subunit-knockout mice. All the tissue embedment was performed by the Research Histology Core at the University of Virginia.

GRANTS

This work was supported by National Heart, Lung, and Blood Institute Grants HL-53318 and HL-72864 (to B. R. Duling), American Heart Association Postdoctoral Fellowship Grant 0325730U (to X. F. Figueroa), a grant from the Vicerrectoría Adjunta de Investigación y Doctorado de la Pontificia Universidad Católica de Chile (to X. F. Figueroa), and Fondo Nacional de Desarrollo Científico y Tecnológico Grant 11060289 (to X. F. Figueroa). K. P. Campbell is an investigator of the Howard Hughes Medical Institute and is supported by the Muscular Dystrophy Association.

REFERENCES

1. Abderrahmane A, Salvail D, Dumoulin M, Garon J, Cadieux A, Rousseau E. Direct activation of K_{Ca} channel in airway smooth muscle by nitric oxide: involvement of a nitrothiosylation mechanism? *Am J Respir Cell Mol Biol* 19: 485–497, 1998.
2. Bossu JL, Elhamedani A, Feltz A. Voltage-dependent calcium entry in confluent bovine capillary endothelial cells. *FEBS Lett* 299: 239–242, 1992.
3. Bossu JL, Feltz A, Rodeau JL, Tanzi F. Voltage-dependent transient calcium currents in freshly dissociated capillary endothelial cells. *FEBS Lett* 255: 377–380, 1989.
4. Brenner R, Perez GJ, Bonev AD, Eckman DM, Kosek JC, Wiler SW, Patterson AJ, Nelson MT, Aldrich RW. Vasoregulation by the β_1 -subunit of the calcium-activated potassium channel. *Nature* 407: 870–876, 2000.
5. Budel S, Bartlett IS, Segal SS. Homocellular conduction along endothelium and smooth muscle of arterioles in hamster cheek pouch: unmasking an NO wave. *Circ Res* 93: 61–68, 2003.
6. Budel S, Schuster A, Stergiopoulos N, Meister JJ, Beny JL. Role of smooth muscle cells on endothelial cell cytosolic free calcium in porcine coronary arteries. *Am J Physiol Heart Circ Physiol* 281: H1156–H1162, 2001.
7. Buga GM, Ignarro LJ. Electrical-field stimulation causes endothelium-dependent and nitric oxide-mediated relaxation of pulmonary artery. *Am J Physiol Heart Circ Physiol* 262: H973–H979, 1992.
8. Campbell WB, Gauthier KM. What is new in endothelium-derived hyperpolarizing factors? *Curr Opin Nephrol Hypertens* 11: 177–183, 2002.
9. Cestele S, Catterall WA. Molecular mechanisms of neurotoxin action on voltage-gated sodium channels. *Biochimie* 82: 883–892, 2000.
10. Chen CC, Lamping KG, Nuno DW, Barresi R, Prouty SJ, Lavoie JL, Cribbs LL, England SK, Sigmund CD, Weiss RM, Williamson RA, Hill JA, Campbell KP. Abnormal coronary function in mice deficient in α_{1H} T-type Ca^{2+} channels. *Science* 302: 1416–1418, 2003.
11. Crane GJ, Neild TO, Segal SS. Contribution of active membrane processes to conducted hyperpolarization in arterioles of hamster cheek pouch. *Microcirculation* 11: 425–433, 2004.
12. De Wit C, Roos F, Bolz SS, Kirchhoff S, Kruger O, Willecke K, Pohl U. Impaired conduction of vasodilation along arterioles in connexin40-deficient mice. *Circ Res* 86: 649–655, 2000.
13. Dora KA, Doyle MP, Duling BR. Elevation of intracellular calcium in smooth muscle causes endothelial cell generation of NO in arterioles. *Proc Natl Acad Sci USA* 94: 6529–6534, 1997.
14. Doyle MP, Duling BR. Acetylcholine induces conducted vasodilation by nitric oxide-dependent and -independent mechanisms. *Am J Physiol Heart Circ Physiol* 272: H1364–H1371, 1997.
15. Ellerkmann RK, Remy S, Chen J, Sochivko D, Elger CE, Urban BW, Becker A, Beck H. Molecular and functional changes in voltage-dependent Na^+ channels following pilocarpine-induced status epilepticus in rat dentate granule cells. *Neuroscience* 119: 323–333, 2003.
16. Emerson GG, Neild TO, Segal SS. Conduction of hyperpolarization along hamster feed arteries: augmentation by acetylcholine. *Am J Physiol Heart Circ Physiol* 283: H102–H109, 2002.
17. Emerson GG, Segal SS. Electrical activation of endothelium evokes vasodilation and hyperpolarization along hamster feed arteries. *Am J Physiol Heart Circ Physiol* 280: H160–H167, 2001.
18. Figueroa XF, Isakson BE, Duling BR. Connexins: gaps in our knowledge of vascular function. *Physiology Bethesda* 19: 277–284, 2004.
19. Figueroa XF, Isakson BE, Duling BR. Vascular gap junctions in hypertension. *Hypertension* 48: 804–811, 2006.
20. Figueroa XF, Paul DL, Simon AM, Goodenough DA, Day KH, Damon DN, Duling BR. Central role of connexin40 in the propagation of electrically activated vasodilation in mouse cremasteric arterioles in vivo. *Circ Res* 92: 793–800, 2003.
21. Fisher AB, Al Mehdi AB, Manevich Y. Shear stress and endothelial cell activation. *Crit Care Med* 30: S192–S197, 2002.
22. Fleming I. Cytochrome P450 epoxigenases as EDHF synthase(s). *Pharmacol Res* 49: 525–533, 2004.
23. Frank GW, Bevan JA. Electrical stimulation causes endothelium-dependent relaxation in lung vessels. *Am J Physiol Heart Circ Physiol* 244: H793–H798, 1983.
24. Geary GG, Maeda G, Gonzalez RR Jr. Endothelium-dependent vascular smooth muscle relaxation activated by electrical field stimulation. *Acta Physiol Scand* 160: 219–228, 1997.
25. Gordienko DV, Tsukahara H. Tetrodotoxin-blockable depolarization-activated Na^+ currents in a cultured endothelial cell line derived from rat interlobar artery and human umbilical vein. *Pflügers Arch* 428: 91–93, 1994.
26. Gosling M, Harley SL, Turner RJ, Carey N, Powell JT. Human saphenous vein endothelial cells express a tetrodotoxin-resistant, voltage-gated sodium current. *J Biol Chem* 273: 21084–21090, 1998.
27. Gustafsson F, Holstein-Rathlou N. Conducted vasomotor responses in arterioles: characteristics, mechanisms and physiological significance. *Acta Physiol Scand* 167: 11–21, 1999.
28. Hansen PB, Jensen BL, Andreassen D, Skott O. Differential expression of T- and L-type voltage-dependent calcium channels in renal resistance vessels. *Circ Res* 89: 630–638, 2001.
29. Hayashi K, Ozawa Y, Wakino S, Kanda T, Homma K, Takamatsu I, Tatematsu S, Saruta T. Cellular mechanism for mibefradil-induced vasodilation of renal microcirculation: studies in the isolated perfused hydronephrotic kidney. *J Cardiovasc Pharmacol* 42: 697–702, 2003.
30. Hermsmeyer K, Miyagawa K. Protein kinase C mechanism enhances vascular muscle relaxation by the Ca^{2+} antagonist, Ro 40-5967. *J Vasc Res* 33: 71–77, 1996.
31. Jackson WF. Potassium channels in the peripheral microcirculation. *Microcirculation* 12: 113–127, 2005.
32. Lacinova L, Klugbauer N, Hofmann F. Low voltage activated calcium channels: from genes to function. *Gen Physiol Biophys* 19: 121–136, 2000.
33. Lee JH, Gomora JC, Cribbs LL, Perez-Reyes E. Nickel block of three cloned T-type calcium channels: low concentrations selectively block α_{1H} . *Biophys J* 77: 3034–3042, 1999.
34. Lew MJ, Rivers RJ, Duling BR. Arteriolar smooth muscle responses are modulated by an intramural diffusion barrier. *Am J Physiol Heart Circ Physiol* 257: H10–H16, 1989.
35. Manabe I, Owens GK. Recruitment of serum response factor and hyperacetylation of histones at smooth muscle-specific regulatory regions during differentiation of a novel P19-derived in vitro smooth muscle differentiation system. *Circ Res* 88: 1127–1134, 2001.
36. Moosmang S, Haider N, Bruderl B, Welling A, Hofmann F. Antihypertensive effects of the putative T-type calcium channel antagonist mibefradil are mediated by the L-type calcium channel $Ca_v1.2$. *Circ Res* 98: 105–110, 2006.
37. Neild TO, Crane GJ. Cellular coupling and conducted vasomotor responses. *Clin Exp Pharmacol Physiol* 29: 626–629, 2002.
38. Nilius B, Droogmans G. Ion channels and their functional role in vascular endothelium. *Physiol Rev* 81: 1415–1459, 2001.
39. Nilius B, Prenen J, Kamouchi M, Viana F, Voets T, Droogmans G. Inhibition by mibefradil, a novel calcium channel antagonist, of Ca^{2+} - and volume-activated Cl^- channels in macrovascular endothelial cells. *Br J Pharmacol* 121: 547–555, 1997.
40. Ohashi M, Satoh K, Itoh T. Acetylcholine-induced membrane potential changes in endothelial cells of rabbit aortic valve. *Br J Pharmacol* 126: 19–26, 1999.
41. Papassotiriou J, Kohler R, Prenen J, Krause H, Akbar M, Eggermont J, Paul M, Distler A, Nilius B, Hoyer J. Endothelial K^+ channel lacks the Ca^{2+} sensitivity-regulating β -subunit. *FASEB J* 14: 885–894, 2000.
42. Patterson AJ, Henrie-Olson J, Brenner R. Vasoregulation at the molecular level: a role for the β_1 -subunit of the calcium-activated potassium (BK) channel. *Trends Cardiovasc Med* 12: 78–82, 2002.

43. **Potocnik SJ, Murphy TV, Kotecha N, Hill MA.** Effects of mibefradil and nifedipine on arteriolar myogenic responsiveness and intracellular Ca^{2+} . *Br J Pharmacol* 131: 1065–1072, 2000.
44. **Prorock AJ, Hafezi-Moghadam A, Laubach VE, Liao JK, Ley K.** Vascular protection by estrogen in ischemia-reperfusion injury requires endothelial nitric oxide synthase. *Am J Physiol Heart Circ Physiol* 284: H133–H140, 2003.
45. **Rivers RJ, Duling BR.** Arteriolar endothelial cell barrier separates two populations of muscarinic receptors. *Am J Physiol Heart Circ Physiol* 262: H1311–H1315, 1992.
46. **Scholz A, Vogel W.** Tetrodotoxin-resistant action potentials in dorsal root ganglion neurons are blocked by local anesthetics. *Pain* 89: 47–52, 2000.
47. **Segal SS.** Integration of blood flow control to skeletal muscle: key role of feed arteries. *Acta Physiol Scand* 168: 511–518, 2000.
48. **Segal SS, Damon DN, Duling BR.** Propagation of vasomotor responses coordinates arteriolar resistances. *Am J Physiol Heart Circ Physiol* 256: H832–H837, 1989.
49. **Segal SS, Duling BR.** Communication between feed arteries and microvessels in hamster striated muscle: segmental vascular responses are functionally coordinated. *Circ Res* 59: 283–290, 1986.
50. **Segal SS, Duling BR.** Conduction of vasomotor responses in arterioles: a role for cell-to-cell coupling. *Am J Physiol Heart Circ Physiol* 256: H838–H845, 1989.
51. **Shimokawa H, Morikawa K.** Hydrogen peroxide is an endothelium-derived hyperpolarizing factor in animals and humans. *J Mol Cell Cardiol* 39: 725–732, 2005.
52. **Siegl D, Koeppen M, Wolfe SE, Pohl U, de Wit C.** Myoendothelial coupling is not prominent in arterioles within the mouse cremaster microcirculation in vivo. *Circ Res* 97: 781–788, 2005.
53. **Sullivan JC, Davison CA.** Effect of age on electrical field stimulation (EFS)-induced endothelium-dependent vasodilation in male and female rats. *Cardiovasc Res* 50: 137–144, 2001.
54. **Tang CM, Presser F, Morad M.** Amiloride selectively blocks the low threshold (T) calcium channel. *Science* 240: 213–215, 1988.
55. **Traub O, Ishida T, Ishida M, Tupper JC, Berk BC.** Shear stress-mediated extracellular signal-regulated kinase activation is regulated by sodium in endothelial cells. Potential role for a voltage-dependent sodium channel. *J Biol Chem* 274: 20144–20150, 1999.
56. **Vanbavel E, Sorop O, Andreasen D, Pfaffendorf M, Jensen BL.** Role of T-type calcium channels in myogenic tone of skeletal muscle resistance arteries. *Am J Physiol Heart Circ Physiol* 283: H2239–H2243, 2002.
57. **Vinet R, Vargas FF.** L- and T-type voltage-gated Ca^{2+} currents in adrenal medulla endothelial cells. *Am J Physiol Heart Circ Physiol* 276: H1313–H1322, 1999.
58. **Walsh KB, Wolf MB, Fan J.** Voltage-gated sodium channels in cardiac microvascular endothelial cells. *Am J Physiol Heart Circ Physiol* 274: H506–H512, 1998.
59. **Wang SY, Wang GK.** Voltage-gated sodium channels as primary targets of diverse lipid-soluble neurotoxins. *Cell Signal* 15: 151–159, 2003.
60. **Wang X, van Breemen C.** Depolarization-mediated inhibition of Ca^{2+} entry in endothelial cells. *Am J Physiol Heart Circ Physiol* 277: H1498–H1504, 1999.
61. **Wei Z, Manevich Y, Al Mehdi AB, Chatterjee S, Fisher AB.** Ca^{2+} flux through voltage-gated channels with flow cessation in pulmonary microvascular endothelial cells. *Microcirculation* 11: 517–526, 2004.
62. **Welsh DG, Segal SS.** Endothelial and smooth muscle cell conduction in arterioles controlling blood flow. *Am J Physiol Heart Circ Physiol* 274: H178–H186, 1998.
63. **Wu S, Haynes J Jr, Taylor JT, Obiako BO, Stubbs JR, Li M, Stevens T.** $Ca_v3.1$ (α_{1G}) T-type Ca^{2+} channels mediate vaso-occlusion of sickled erythrocytes in lung microcirculation. *Circ Res* 93: 346–353, 2003.
64. **Wu S, Zhang M, Vest PA, Bhattacharjee A, Liu L, Li M.** A mibefradil metabolite is a potent intracellular blocker of L-type Ca^{2+} currents in pancreatic β -cells. *J Pharmacol Exp Ther* 292: 939–943, 2000.
65. **Xia J, Duling BR.** Electromechanical coupling and the conducted vasomotor response. *Am J Physiol Heart Circ Physiol* 269: H2022–H2030, 1995.
66. **Yakubu MA, Leffler CW.** L-type voltage-dependent Ca^{2+} channels in cerebral microvascular endothelial cells and ET-1 biosynthesis. *Am J Physiol Cell Physiol* 283: C1687–C1695, 2002.
67. **Yashiro Y, Duling BR.** Integrated Ca^{2+} signaling between smooth muscle and endothelium of resistance vessels. *Circ Res* 87: 1048–1054, 2000.
68. **Yunker AM.** Modulation and pharmacology of low voltage-activated (“T-type”) calcium channels. *J Bioenerg Biomembr* 35: 577–598, 2003.
69. **Yunker AM, McEnery MW.** Low-voltage-activated (“T-type”) calcium channels in review. *J Bioenerg Biomembr* 35: 533–575, 2003.
70. **Zhou C, Wu S.** T-type calcium channels in pulmonary vascular endothelium. *Microcirculation* 13: 645–656, 2006.